sustainability

MDPI

Article

Seismicity and Stress State in the Ryukyu Islands Subduction Zone

Zhuojuan Xie [1], Enhui Wang [2] and Yuejun Lyu [1,*]

[1] National Institute of Natural Hazards, Ministry of Emergency Management of China, Beijing 100085, China
[2] Sinopec Shengli Oilfield Company, Dongying 257100, China
* Correspondence: yuejunlv@ninhm.ac.cn

Abstract: Based on the newly compiled and mostly complete unified earthquake catalogue for China's seas and adjacent areas, further information was obtained about the structural shape and dip angle of the Benioff zone in the Ryukyu Islands subduction zone during the different subduction stages. In addition, using the damped regional stress tensor inversion method, we were able to investigate the complex stress field characteristics and the dynamic significance of the shallow and intermediate earthquakes in the Ryukyu Islands subduction zone. The results show that the tectonic stress field of the Ryukyu Islands subduction zone was extensional along the subduction direction in the northern area of the Tokara Strait and was compressional along the subduction direction in the southern area of the Tokara Strait. The R value of the shallow stress field of the Okinawa Trough was low, and the σ_3 was stable in the NNW direction with a small dip angle (>30°). The type of stress field in the shallow part of the Okinawa Trough transitioned from strike-slip type to normal fault type from north to south, reflecting the difference in the degree of development of the trough, and the southern segment of the trough began to transform into the expansion stage. The northeastern portion of the study area and southeast Taiwan constituted the high R value (0.68–0.87) region where the σ_2 had tensile components. The stress state was biaxial tension–uniaxial compression, and the principal compressive stress was determined to be in the SEE direction with a large dip angle (>30°). The σ_1 in northeast Taiwan exhibited a nearly vertical (>60°) plunge, while the σ_2 and σ_3 were nearly horizontal. The σ_2 was thrust in the ENE–WSW direction, and the σ_3 was extended in the NNW direction. Through this research, a greater understanding has been gained of the seismicity characteristics and shape of the Ryukyu Islands subduction zone. Supplementary research has also been completed on the focal mechanism solution and stress field of the Ryukyu Islands subduction zone. Finally, this research is important for earthquake hazard analysis and earthquake engineering safety evaluation in this area.

Keywords: Ryukyu Islands subduction zone; earthquake; seismicity; dip angle; stress field

check for updates

Citation: Xie, Z.; Wang, E.; Lyu, Y. Seismicity and Stress State in the Ryukyu Islands Subduction Zone. *Sustainability* **2022**, *14*, 15146. https://doi.org/10.3390/su142215146

Academic Editors: Yang Wu, Norimasa Yoshimoto and Rongtao Yan

Received: 8 October 2022
Accepted: 14 November 2022
Published: 15 November 2022

1. Introduction

Subduction zones are the most seismically active areas on Earth, and most of the major earthquakes in the world occur in these areas [1,2]. The Ryukyu Islands subduction zone is one of the subduction zones of the Circum-Pacific Plate, extending from the Izu Peninsula in Japan in the north to the east of Taiwan Island in the southwest. Due to the movements of and interactions between the Eurasian Plate, the Western Pacific Plate, and the Philippine Sea Plate, the seismic activity is frequent and intense. There have been many strong earthquakes with magnitudes of seven or greater, and the seismic activity is still very high. The occurrence of a strong earthquake and related tsunami could cause huge disaster losses in the eastern coastal areas, eastern sea areas, and coastal construction engineering areas of China [3–9]. Therefore, understanding and studying the seismicity characteristics, stress state, and their relationships with the tectonic environment of the Ryukyu Islands subduction zone can provide a scientific basis for the division of the seismogenic structures in this region, the division of potential seismic source zones in the shallow and mid-deep regions of this plate boundary subduction zone, and the determination of the seismicity parameters. This research is fundamental for seismic hazard analysis and seismic zoning in this region.

Scholars have conducted research on the distribution of the seismic activity in the Ryukyu Islands subduction zone. Katsumat and Sykes [10] first studied the seismicity of the Ryukyu region using a seismic dataset for 1961–1967. It has been proposed that there is a seismic gap between 24–25° N and 126–128° E in the Ryukyu Islands subduction zone where a major earthquake may occur in the future. It has also been noted that the mid-deep earthquakes in the Ryukyu Islands subduction zone are distributed within a thin belt with a thickness of 50 km and a northwest inclination of 35° to 45°. Fitch [11] supplemented the seismic dataset created by Katsumat and Sykes with data for 1968–1970 to study the seismicity in the Ryukyu Islands subduction zone. Shiono et al. [12] used data for earthquakes with magnitudes of 5 or higher during 1964–1975 obtained from the International Seismological Center (ISC) to study the seismicity of the shallow to medium-deep earthquakes in the Kyushu–Ryukyu Island Arc in detail. These studies provided further support for the existence of the seismic gap (24–25° N, 126–128° E), and revealed the shape and dip of the Ryukyu Islands subduction zone and its Wadati–Benioff zone. Zang et al. [13] combined seismic data for 1966–1982 from the ISC and the China Seismic Network, studied the seismic distribution characteristics of the Ryukyu Island Arc and the Okinawa Trough, and discussed the shape of the Benioff zone in the different segments. The results of the above studies have improved our understanding of the spatial distribution of the seismic activity in the Ryukyu Islands subduction zone. However, the seismic data that were used in these previous studies are relatively old, and they do not reflect the seismic activity characteristics of the present Ryukyu Islands area. Through research conducted on the key technologies for China's seismic zoning in sea areas, a recent and relatively complete unified earthquake catalogue for China's seas and adjacent areas has been compiled [14]. It is necessary to use the latest research results and data to analyze the spatial, temporal, and intensity distribution characteristics of the seismic activity in the Ryukyu Islands subduction zone, as well as the spatial and focal depth distribution characteristics of the seismic activity in this area. Using these recent data, it is possible to gain a better understanding of the structure of the subduction zone and the dip of the Benioff zone in the different regions and to further investigate the complex stress field characteristics and dynamic significance of the shallow and intermediate earthquakes in the Ryukyu subduction zone. Through this research, we gained a greater understanding of the seismicity characteristics and shape of the Ryukyu Islands subduction zone. Supplementary research has also been completed on the focal mechanism solution and stress field of the Ryukyu Islands subduction zone. This research is important for the earthquake hazard analysis and earthquake engineering safety evaluation in this area.

2. Seismotectonic Background of the Ryukyu Islands Subduction Zone

The Ryukyu Islands subduction zone was created by the convergence of continental and oceanic plates and is part of the subduction zone system formed by the Western Pacific and Philippine Sea plates. The Philippine Sea Plate is subducting toward the Eurasian Plate along the Ryukyu Trench at a rate of about 6 cm per year [15], and is subducting underneath the Ryukyu Island Arc. A trench–arc–basin system consisting of the Ryukyu Trench, the Ryukyu Island Arc, and the Okinawa Trough back-arc basin has formed on the edge of the Western Pacific Ocean and the southeastern side of the East China Sea (Figure 1), and it is an important part of the Western Pacific trench–arc–basin system.

The Ryukyu Trench is the boundary between the Eurasian Plate and the Philippine Sea Plate. The west slope of the trench is composed of the continental Ryukyu Island Arc, and the east slope is composed of the oceanic crust of the Philippine Sea Plate. The northeastern end of the Ryukyu Island Arc starts at the southern end of Kyushu, Japan, and its southwestern end is located east of Taiwan Island, China. It is a 1200 km long island chain composed of more than 100 islands. It is separated from the edge of the continental plate in eastern China due to the extension of the Okinawa Trough, and its eastern side dips steeply toward the Ryukyu Trench. The back-arc basin of the Okinawa Trough is bounded by the Diaoyu Island Belt Uplift and the Ryukyu Belt Uplift. It is generally an arc protruding to the southeast, with a length of about 1200 km. It is narrow at the southwest end and widens toward the northeast, and the width changes greatly, from 72 km to 160 km.

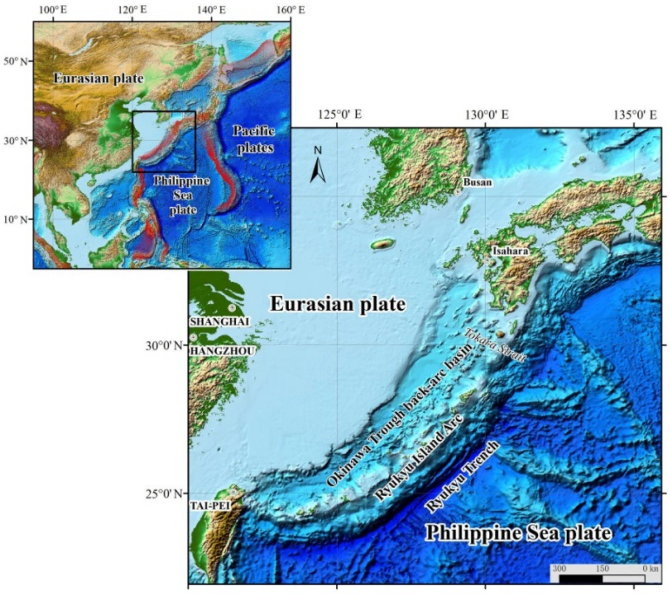

Figure 1. The tectonic background of the Ryukyu Islands subduction zone.

3. Characteristics of the Seismic Activity in the Ryukyu Islands Subduction Zone

The seismic data used in this study were obtained from the latest and relatively complete unified earthquake catalogue of China's seas and adjacent areas [14].

3.1. Epicenter Distribution

Data for a total of 9335 earthquake events with magnitudes of greater than M2.0 in the Ryukyu Islands subduction zone were collected. Among them were two earthquakes with magnitudes of greater than 8.0, 37 earthquakes with magnitudes of 7.0–7.9, 214 earthquakes with magnitudes of 6.0–6.9, 858 earthquakes with magnitudes of 5.0–5.9, 929 earthquakes with magnitudes of 4.7–4.9, 2093 earthquakes with magnitudes of 4.0–4.6, 4489 earthquakes with magnitudes of 3.0–3.9, and 713 earthquakes with magnitudes of 2.0–2.9. Based on the frequency of each magnitude bin, it is apparent that a considerable number of earthquakes with magnitudes of less than M3.0 are missing, and some earthquakes with magnitudes of M3.0–3.9 are missing, while the records of earthquakes with magnitudes greater than M4.0 are relatively complete. Thus, the seismic data for the $M \geq 4.0$ earthquakes were used to determine the distribution of the earthquake epicenters and to analyze the distribution characteristics of the focal depths and times of the earthquakes in the Ryukyu Islands subduction zone.

Based on the collected seismic data, a distribution map of the active structures and the earthquake epicenters in the Ryukyu Islands subduction zone is shown in Figure 2. The Ryukyu Islands subduction zone is NE trending, with a total length of more than 1000 km. Most of the earthquakes are distributed in the seismic zone on the west side of the Ryukyu Trench. The seismic activity in the Ryukyu Islands subduction zone is very strong. There have been multiple earthquakes with magnitudes of 7 or greater. In modern times, this subduction zone has been intensely active. The earthquakes with magnitudes of 7 or greater have mainly occurred in the eastern and northeastern parts of Taiwan Island, the eastern side of Kyushu Island, the central section of the Ryukyu Island Arc, and the central and southern sections of the back-arc basin of the Okinawa Trough. The depth distribution of the earthquakes in the Ryukyu Islands subduction zone gradually deepens from shallow earthquakes to intermediate earthquakes in the Ryukyu Trough to the west to the Ryukyu Island Arc to the back-arc basin of the Okinawa Trough. As can be seen from Figure 2, the focal depths of the mid-deep earthquakes can be further divided into two levels: 175 km $\leq$ H < 300 km (red in Figure 2) and 70 km $\leq$ H < 175 km (green in Figure 2). It appears that the focal depths are deeper closer to the western edge of the Okinawa Trough, and the distribution of the focal depths is obviously layered from east to west.

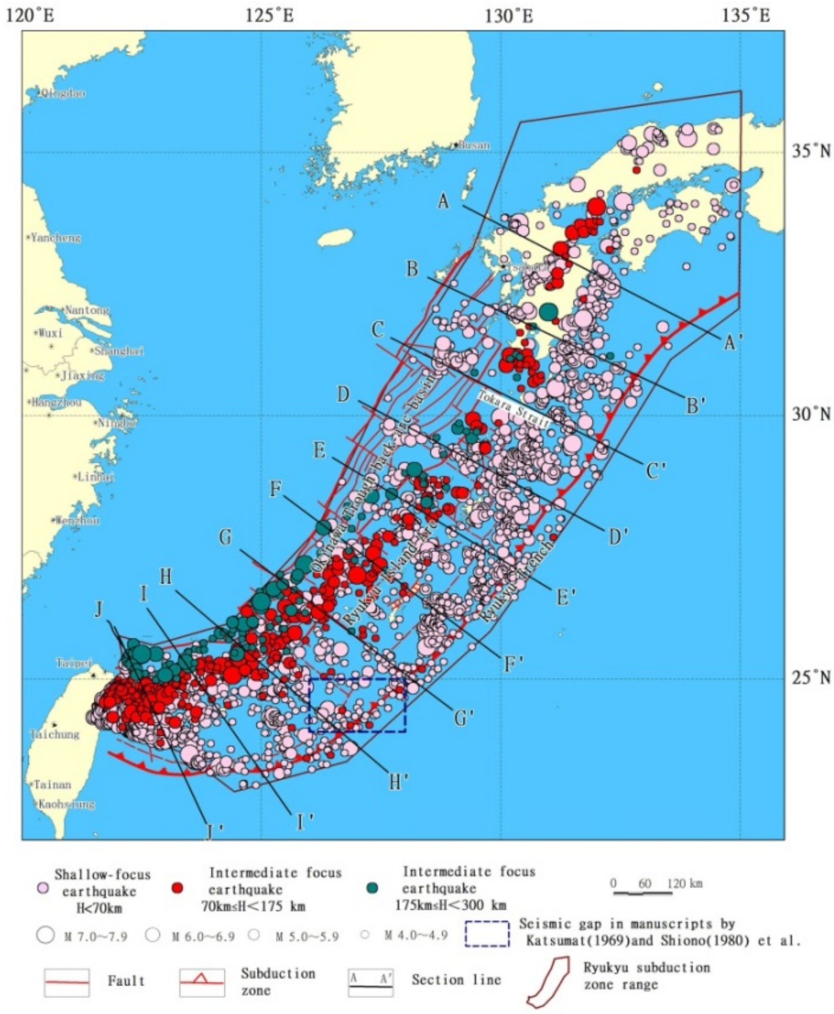

Figure 2. Seismotectonics and distribution of the earthquake epicenters in the Ryukyu Islands subduction zone [10,12].

Using the seismic data for 1961–1967, Katsumat and Sykes [10] proposed that there is a seismic gap between 24–25° N and 126–128° E in the Ryukyu Islands subduction zone where a major earthquake may occur in the future. Subsequently, further studies conducted by Shiono et al. [12] and Zang et al. [13] substantiated the existence of this seismic gap (blue dotted box in Figure 2). By analyzing the current seismic data in this seismic gap, as well as the distribution of the earthquake epicenters in the seismic gap shown in Figure 2, we found that 63 earthquakes with magnitudes greater than 4.0 have been detected in this seismic gap since 1990, all of which were shallow earthquakes. Among these, there have been five destructive earthquakes with magnitudes of 5.0 or greater, and the largest earthquake (magnitude of 6.2) occurred on 9 May 2017. The seismic activity in this area is more active than before; however, compared with other areas in the Ryukyu Islands subduction zone, the frequency of earthquakes is low and the magnitudes are relatively low.

3.2. Focal Depth Distribution

To further analyze the distribution characteristics of the focal depths in the Ryukyu Islands subduction zone and to understand the changes in the structural shape and dip angle of the Benioff zone in the different sections of the subduction zone, 10 different cross-sections of the Ryukyu Islands subduction zone were established from north to south: AA′, BB′, CC′, DD′, EE′, FF′, GG′, HH′, II′, and JJ′ (Figure 3). Each cross-section was nearly 600 km long and had a projected width of 150 km. The locations of the cross-section are shown in Figure 2.

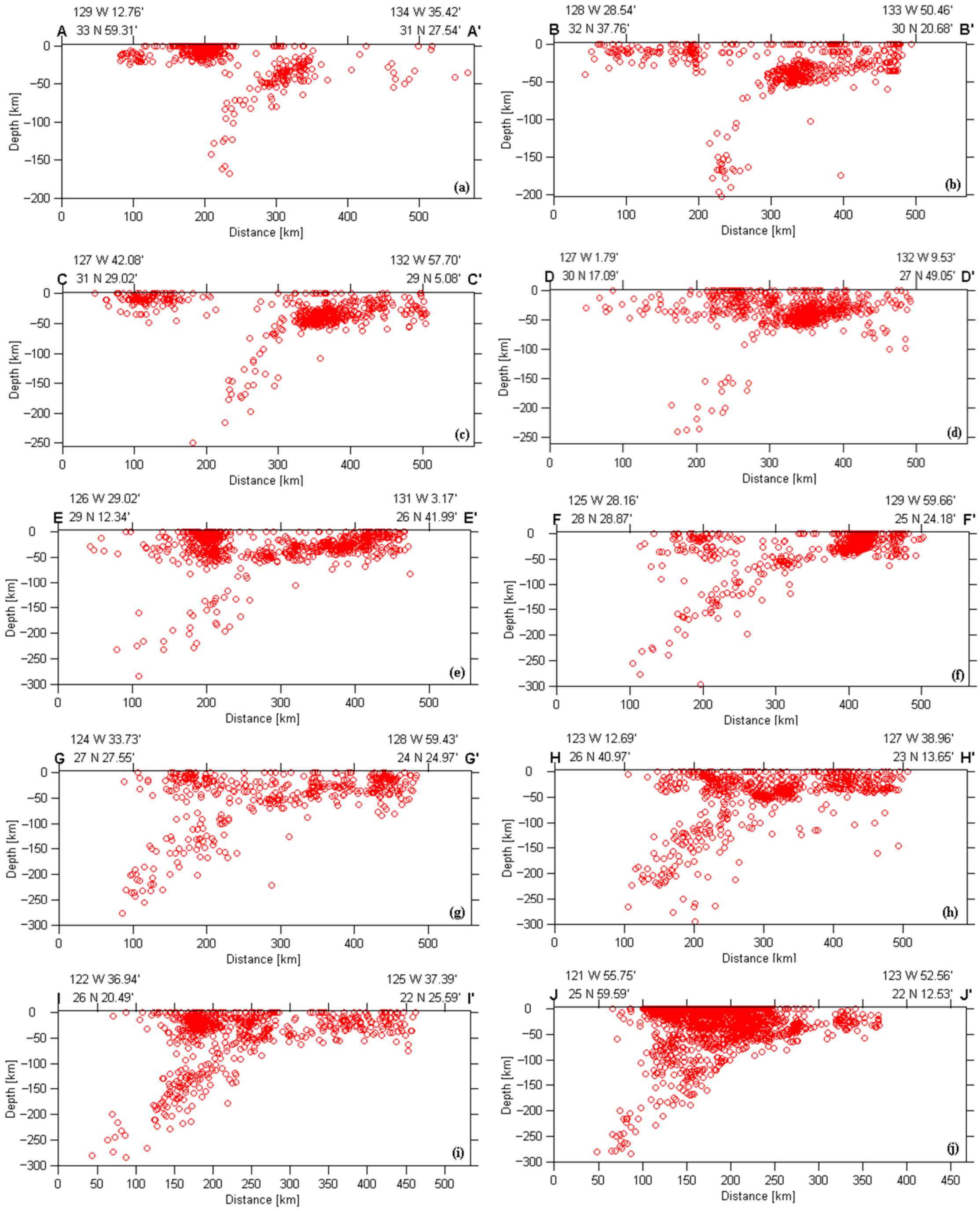

Figure 3. Seismic focal depth profiles of different sections of the Ryukyu Islands subduction zone: (**a**) AA′; (**b**) BB′; (**c**) CC′; (**d**) DD′; (**e**) EE′; (**f**) FF′; (**g**) GG′; (**h**) HH′; (**i**) II′; and (**j**) JJ′.

The seismic activity in the Ryukyu Islands subduction zone is mainly divided into two regions. The first region is composed of the shallow seismic activity, which is widely distributed in the Ryukyu Island Arc and the Okinawa Trough (Figures 2 and 3). The second region contains the focal depth zone of the moderate earthquakes with depths of 70–300 km, which is formed by the westward subduction of the Philippine Sea Plate toward the bottom of the Okinawa Trough Basin and the Diaoyu Island Uplift and constitutes the lower layer of the double-layered hypocenter distribution in this area.

Several studies have revealed that the maximum depth of seismicity in Kyushu, Japan, is 200 km, while it is about 270 km in the central and southern parts of the island arc [12,16–18]. According to these studies, the subduction zone has a shallow dip angle of about 30°. North of the Tokala Strait, the curvature is significant at depths of 70–100 km and the dip angle is about 60–70°. In the southern part of the Tukala Strait, the dip angle of the subduction zone is about 50° at depths greater than 100 km [12,17]. The cross-sections of the 10 different segments of the Ryukyu Islands subduction zone created in this study (Figure 3) extend through the Ryukyu Trench and the Ryukyu Island Arc from east to northwest and into the Okinawa Trough back-arc basin. There is a dipping seismic zone here, namely, the Wadati–Benioff zone, which confirms that the Ryukyu Islands subduction zone was formed by the subduction of the Philippine Sea Plate under the Eurasian Plate. This subduction zone reaches a maximum depth of 300 km in the mantle and the subducting plate bends at a depth of about 70 km. The dip angle of the subduction zone is about 20–30° in the upper part of the Ryukyu Trough, about 45° at the Ryukyu Island Arc, and about 45–70° at the lower back-arc basin of the Okinawa Trough. The cross-sections show that the earthquake distribution in the Ryukyu area is characterized by shallow earthquakes in the trench area, which gradually deepen to intermediate earthquakes toward the northwest.

As can be seen from cross-sections AA′ to JJ′, the structure and dip of the Benioff zone in different sections of the Ryukyu Islands subduction zone exhibit obvious differences. In the Kyushu Island area in the northern part of the subduction zone (AA′ and BB′), the maximum depth of the Benioff zone in the mantle is about 200 km. Near the Tokara Strait in the middle of the subduction zone (the Tokara Strait is located between sections CC′ and DD′; Figure 2), the Benioff zone reaches a maximum depth of 250 km in the mantle. In the southern part of the subduction zone under the northeastern part of Taiwan Island (GG′ to JJ′), the Benioff zone reaches a maximum depth of 300 km in the mantle. The subduction dip angles of the Benioff zone in the different segments of the Ryukyu Islands subduction belt are also different. In cross-sections AA′ and BB′ in the northern part of the Tokara Strait, the Benioff zone bends at a depth of approximately 70 km, and the high subduction dip angle decreases. The dip angles in cross-sections AA′ and BB′ are 70° and 73°, respectively. The subduction dip angles in cross-sections CC′ and DD′ are about 50° to 55°, i.e., gentler than those to the north. The shape and dip angle of the Benioff zone south of the Tokara Strait (EE′ to JJ′) are roughly the same, and the dip of the subduction zone is relatively gentle, with dip angles of about 45° to 50°. Generally, the subduction depth of the Ryukyu Islands subduction zone in the mantle gradually increases from north to south, and the subduction dip angle transitions from steep to gentle.

3.3. Temporal Distribution

The temporal distribution of the regional seismicity describes the seismicity in different time periods. According to the magnitude-time (M-T) and strain release curve (E-T) diagrams, the seismicity characteristics of the shallow earthquakes and intermediate earthquakes in the Ryukyu Islands subduction zone since 1890 were analyzed hierarchically (Figure 4). For both shallow earthquakes and intermediate earthquakes, the seismicity of the Ryukyu Islands subduction zone has been fairly active. Due to the accumulation and release of the strain energy, during the past 100 years, the Ryukyu Islands subduction zone has experienced many major release events. Due to the short duration of the historical seismic records for this area, it is difficult to analyze the periodic characteristics of the seismic activity. It is expected that in the next 100 years, the overall level of the seismic activity will be similar to that during the past 100 years, and there is a possibility that earthquakes with magnitudes of 7 or greater will occur in this seismic area.

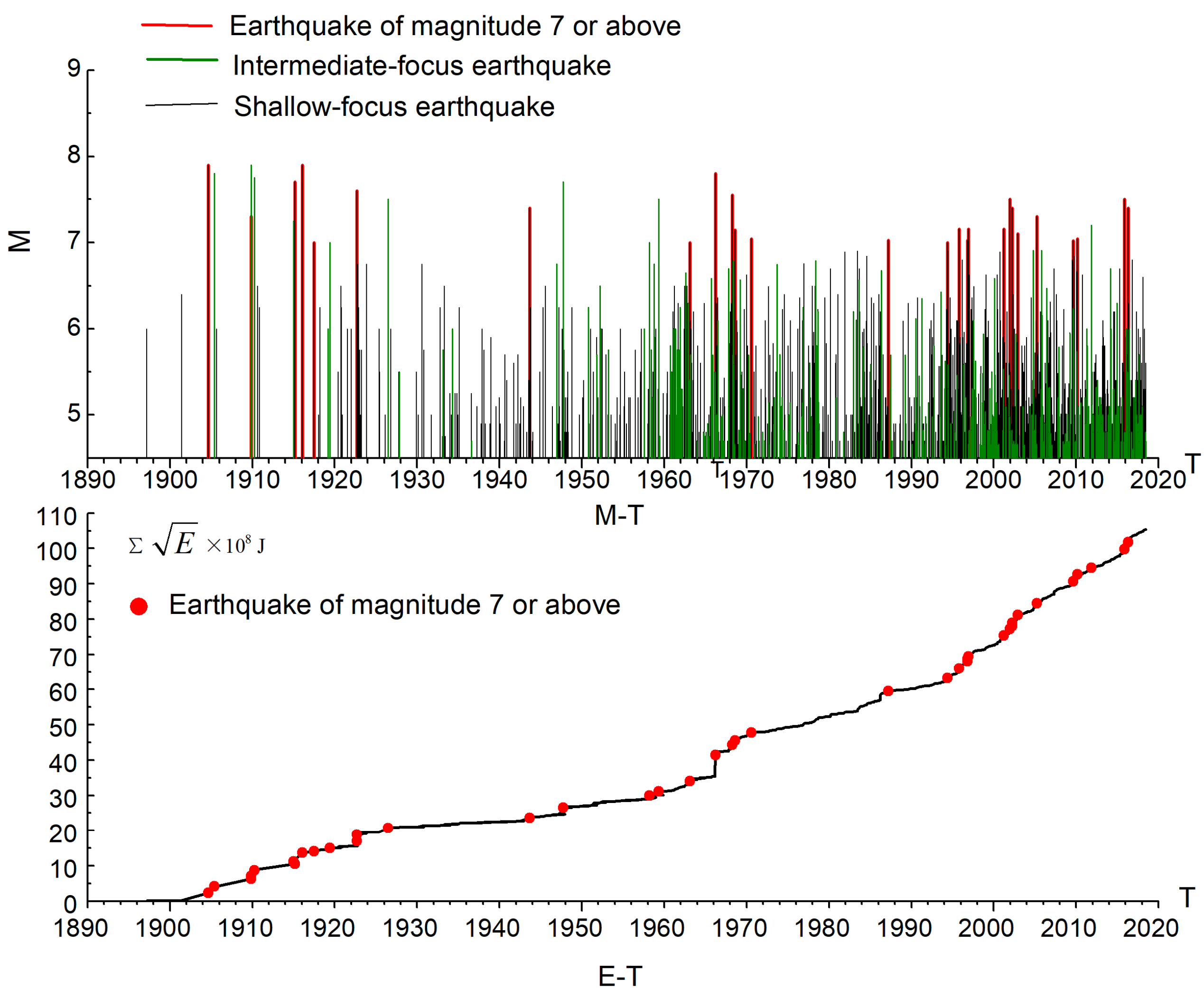

Figure 4. The magnitude-time (M-T) and strain release curves (E-T) for the Ryukyu Islands subduction zone since 1890.

In order to further analyze the temporal distribution characteristics of the different segments of the Ryukyu Islands subduction zone, cross-sections AA′, DD′, GG′, and II′ were selected for analysis (Figure 2). Each section is nearly 600 km long and has a projected width of 300 km. The distributions of the earthquakes over time in the selected cross-sections are shown in Figure 5. It can be seen from Figure 5 that the temporal distributions in the different segments of the subduction zone are clearly different. The earthquakes in the northern and middle segments mostly occurred after 1997, coinciding with the establishment of the national high-sensitivity seismic network Hi-net and the broadband seismograph network F-net in 1997, which cover the entire territory of Japan, including Ishigaki City in the Ryukyu Islands. This is also related to the substantial improvement in earthquake monitoring capabilities since 1997 [14]. The earthquakes in the southern segment, close to Taiwan Island, were denser than in other sections between 1900 and 1996, which is related to the earlier earthquake observation work in Taiwan and the relatively higher seismic monitoring capacity during this period compared to that in the middle and northern segments.

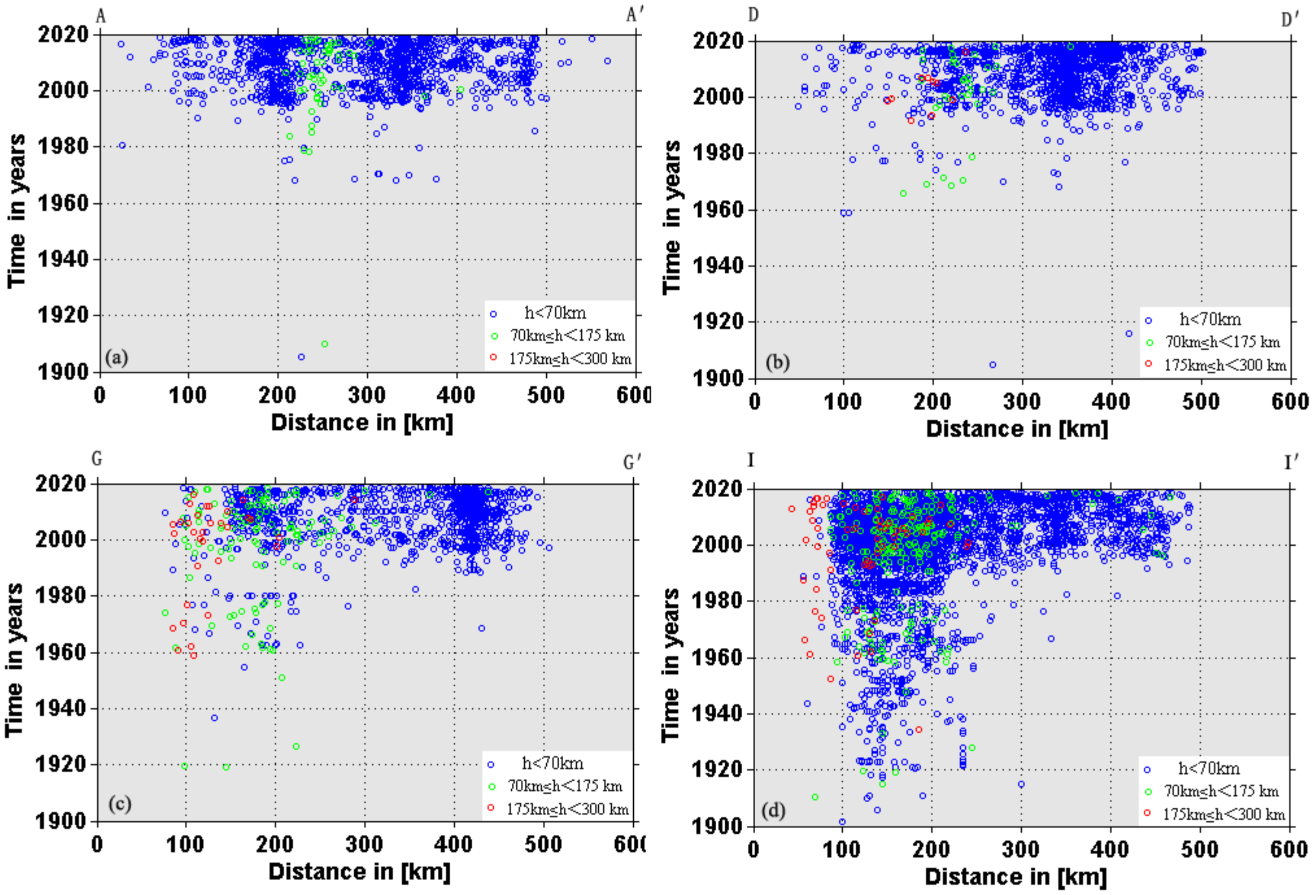

Figure 5. Temporal distributions of the earthquakes in the different sections of the Ryukyu Islands subduction zone: (**a**) AA′; (**b**) DD′; (**c**) GG′; and (**d**) II′.

4. Characteristics of the Tectonic Stress Field

Using the damped area stress tensor inversion method proposed by Hardebeck and Michael [19] and the focal mechanism solution data, 98 grids (14 rows × 7 columns) were generated according to the trend of the Ryukyu Trench (gray dashed line in Figure 6). Each grid represents a 1° × 1° planar grid. The MSATSI software [20] was used to conduct the stress field inversion, and the characteristics of the tectonic stress field of the shallow and intermediate depth sources in the Ryukyu Islands subduction zone were studied.

4.1. Characteristics of the Focal Mechanism Solutions

According to the trend of the Ryukyu Trench, a 1° × 1° planar grid was generated. Figure 7 shows the focal mechanism solution projections in seven vertical sections (AA′, BB′, CC′, DD′, EE′, FF′, and GG′) transverse to the strike of the trench (the positions of the profiles are shown in Figure 6). Cross-sections AA′ to FF′ are parallel to each other, with lengths of about 730 km and projection widths of 200 km. GG′ is perpendicular to the first six sections, with a length of about 1470 km and a projected width of 700 km. In Figure 7, above each section, a topographic map of the seafloor along that section is shown. In Figure 7, the green, red, blue, pink, orange, and black beach balls represent strike-slip, thrust, normal fault, positive strike-slip, reverse strike-slip, and uncertain focal mechanism solutions, respectively. In order to further illustrate the solution distribution of the different focal mechanism solutions, Figure 8 plots the distribution of the different types of focal mechanism solutions in the Ryukyu Islands subduction zone.

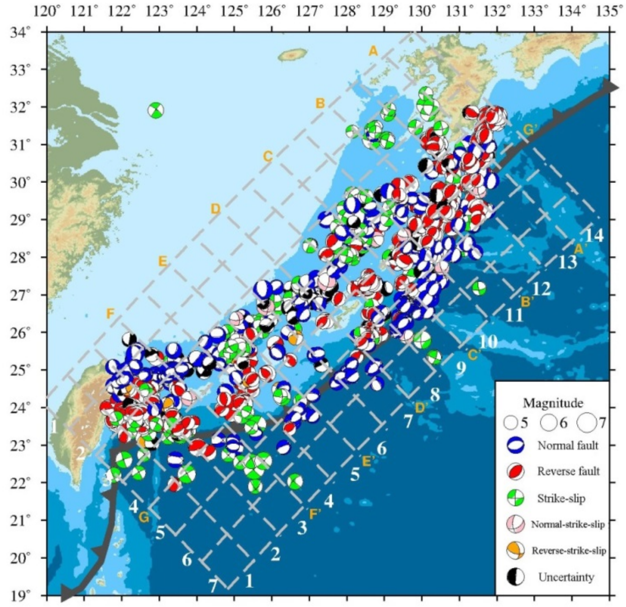

Figure 6. Distribution and grid division of the focal mechanism solutions in the Ryukyu Islands subduction zone. The size of the beach ball in the figure represents the magnitude, and the color represents the type of focal mechanism solution. The gray dashed lines denote the 1° × 1° plane grid.

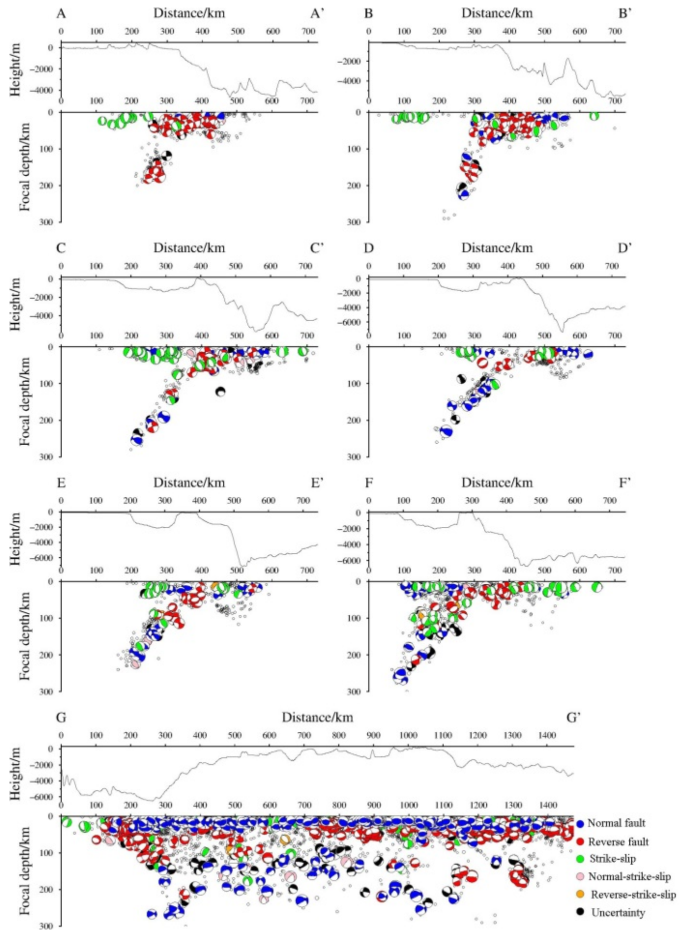

Figure 7. Distribution map of topographic and focal mechanism solutions on the sections of the Ryukyu Islands subduction zone.

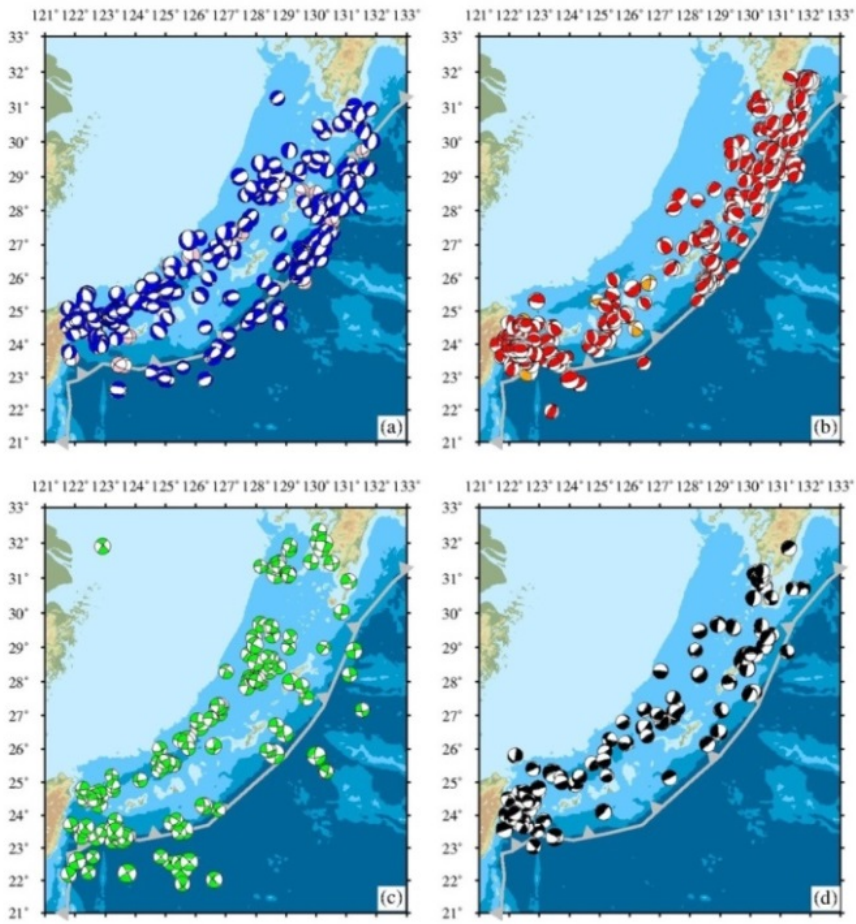

Figure 8. Distribution of focal mechanism solution types in the Ryukyu Islands subduction zone: (**a**) normal fault type; (**b**) reverse fault type; (**c**) strike-slip type; and (**d**) uncertain type.

The thrust earthquakes are mainly distributed along the Ryukyu Island Arc (Figures 6–8). The normal fault type earthquakes are mainly distributed in the periphery of the reverse fault type earthquake accumulation area, that is, along the Ryukyu Trench and the Okinawa Trough. Most of the strike-slip earthquakes are distributed in the Okinawa Trough, and a few are scattered in the southeastern part of the Ryukyu Trench. The normal fault type intermediate focal depth earthquakes are mainly distributed in the middle and southern segments of the Ryukyu Islands subduction zone, and the reverse fault type intermediate focal depth earthquakes are mainly distributed in the northern segment of the Ryukyu Islands subduction zone. The distribution of the normal fault type earthquakes contains a gap within the depth interval of 30–100 km, and the reverse fault type earthquakes are mainly distributed within the depth interval of 0–70 km. The strike-slip type earthquakes are relatively shallow, and they are mainly distributed in the shallow seismic region, concentrated at depths of 0–30 km.

From the focal mechanism solutions and topographic profiles, we can also see the subduction shape and dip angle of the subduction zone in the different segments. Lines 10 and 11 of the grids are centered on the Tokara Strait. The shape of the subduction zone is significantly different on the north and south sides of the Tokara Strait. On the north side, the curvature is significant at a depth of 70–100 km, and the dip angle is about 70–73°. In the southern part, the dip angle of the subduction zone is about 45–55° at depths greater than 100 km. This is consistent with the results of the analysis of the seismic focal depth profiles of the different segments of the Ryukyu Islands subduction zone presented in Section 3.

4.2. Selection of an Optimal Damping Coefficient

In the inversion procedure, the relationship between the data variance and model length is referred to as a trade-off curve, on which there is a mutual counterbalance between the data variance and the model length. The damping parameter e [19] is used to control the relative weights of the variance between the theoretical and observed data and the stress inversion model length. The damping parameter e plays a compromising role, in that a more simplified model has a larger data variance and thus larger inversion errors. In contrast, increasing the relative weight of the data variance reduces the inversion errors, and the model becomes more complex and can even lose the significance of the damping constraints. Usually, the inflection point of the trade-off curve (red solid circle in Figure 9) is the optimal damping coefficient [19,20]. When the coefficient is lower than this relative weight value, increasing the complexity of the model has little effect on improving the inversion error; however, when the relative weight is increased, the model is simplified, and the inversion error will increase. In the stress field inversion of the Ryukyu Islands subduction zone, the optimal damping coefficient was set to 1.3 for both depth ranges, i.e., 0–70 km and 70–300 km (Figure 9).

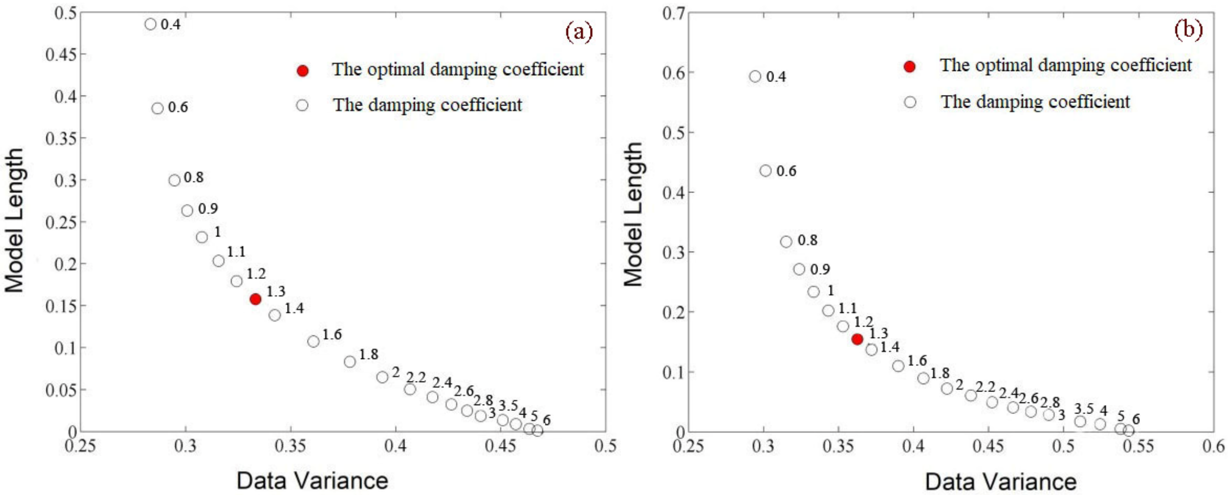

Figure 9. Trade-off curves showing the relationship between the model length and the data variance for the (**a**) shallow (0–70 km); and (**b**) deep (70–300 km) regions.

4.3. Analysis of the Tectonic Stress Field

Through analysis of the inversion results of the stress field in the shallow and deep regions of the Ryukyu Islands subduction zone (Figures 10 and 11, Tables 1 and 2), the dominant direction of the principal compressive stress axis, σ_1, in the shallow region of the study area was determined to be SE, i.e., opposite to the dip direction of the subduction zone. The dominant direction of the principal tensile stress axis, σ_3, was determined to be NW with a large dip angle, which is consistent with the dip direction of the subduction zone. From northeast to southwest, the maximum σ_3 in the shallow region gradually rotates clockwise from NW to NNW, which is perpendicular to the trend of the trench. The maximum σ_1 of the shallow northern-central section (rows 6–14 in the grid) rotates clockwise from ENE to ESE from northwest to southeast (columns 1–7 in the grid), and the dip angle gradually increases. The western edge of the Okinawa Trough (cells in rows 5–13 and columns 1–3) is in the low R value (0.09–0.2) region. The intermediate principal stress axis, σ_2, has a compressive component with a biaxial compression-uniaxial tension stress state. The principal tensile stress was essentially determined. All of the σ_3 in this area is oriented to the NW and the dip angle is generally low (<30°), making it close to horizontal, indicating NW–SE expansion towards the back-arc basin is occurring in the trough, which is consistent with the subduction direction of the Philippine Sea Plate. The northeast section of the study area (cells in rows 11–13 and columns 4–7) and southeast Taiwan constitute the high R value (0.68–0.87) region, in which the σ_2 has tensile components. The stress state is biaxial tension-uniaxial compression, and the principal compressive stress is oriented ESE with a large dip angle (>30°). In addition, the intermediate principal stress axis σ_2 in this area sub-horizontally plunges at a very small dip angle (<11°). The dip angle of the σ_1 increases from 35° to 60° in the direction opposite to the subduction motion. The dip angle of the σ_2 in the cells in rows 8–9 and columns 2–3 is greater than 60°, with a sub-vertical plunge, while the σ_1 and σ_3 are nearly horizontal. The σ_1 is compressional in the ENE–WSW direction, and the σ_3 is extensional in the NNW–SSE direction, i.e., strike-slip type. The σ_1 in northeast Taiwan (cells in rows 3–5 and columns 1–3) has a nearly vertical (>60°) plunge, while the σ_2 and σ_3 are nearly horizontal. The σ_2 is compressional in the ENE–WSW direction, and the σ_3 is extensional in the NNW direction, i.e., normal fault type. The stress type of the Okinawa Trough from north to south in the shallow region transitions from strike-slip type to normal fault type, reflecting the difference in the degree of development of the trough and the transformation of the southern section of the trough into an expansion stage.

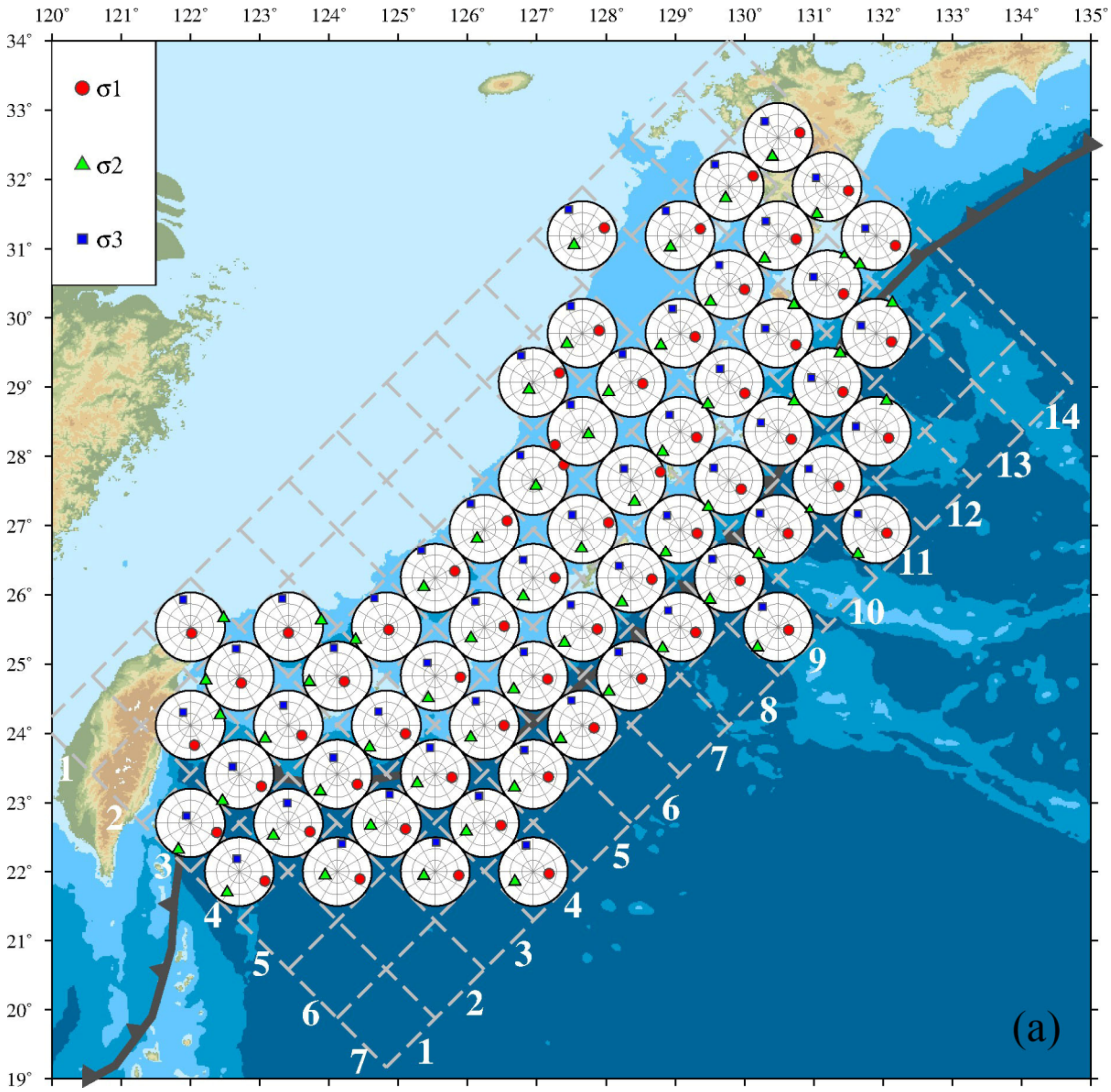

Figure 10. *Cont.*

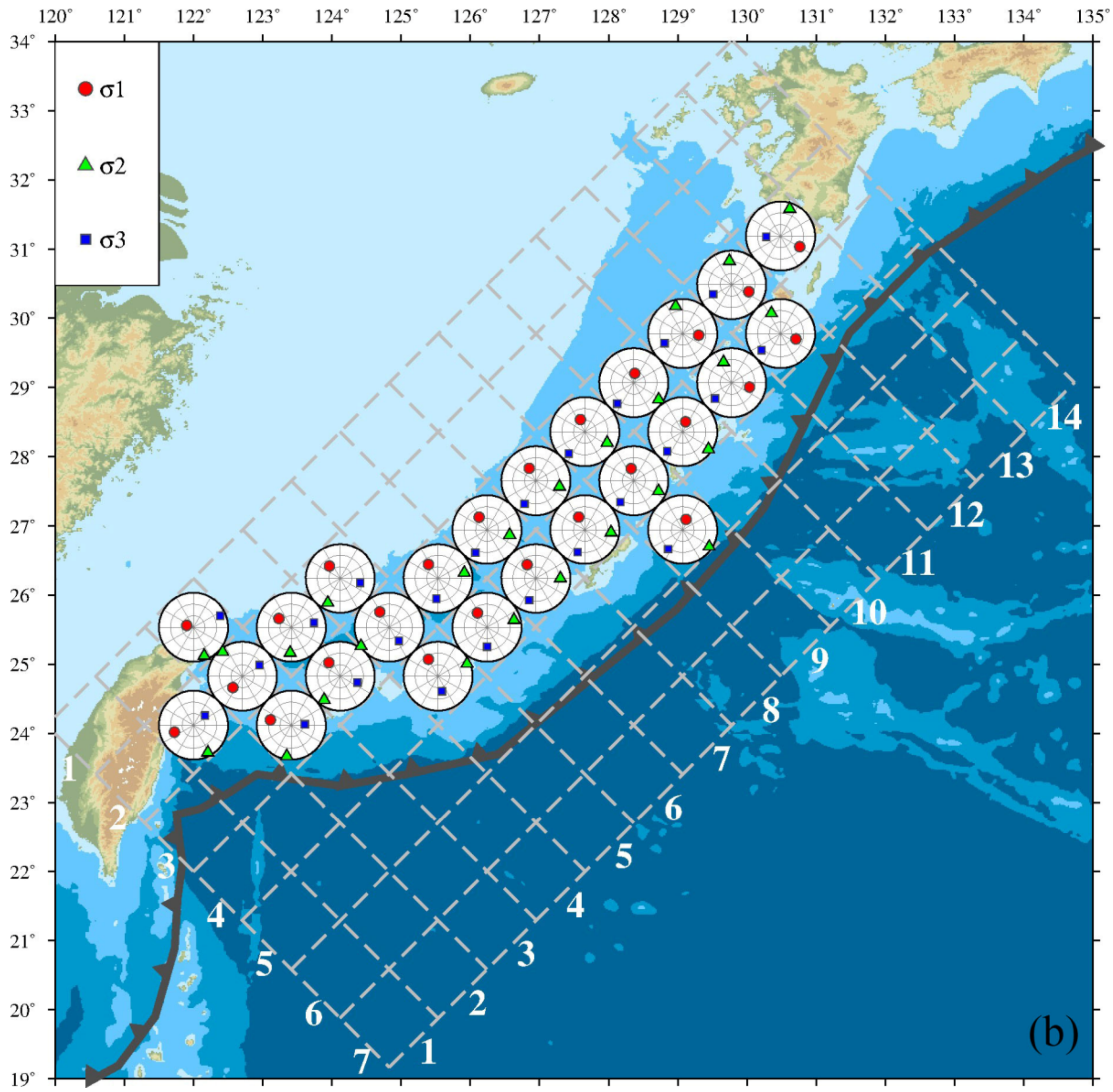

Figure 10. Inversion results of the stress field in the Ryukyu Islands subduction zone (lower hemisphere projection): (**a**) shallow stress field; and (**b**) deep stress field. The σ_1 is the maximum principal compressive stress axis; σ_2 is the intermediate stress axis; and σ_3 is the maximum tensile stress axis.

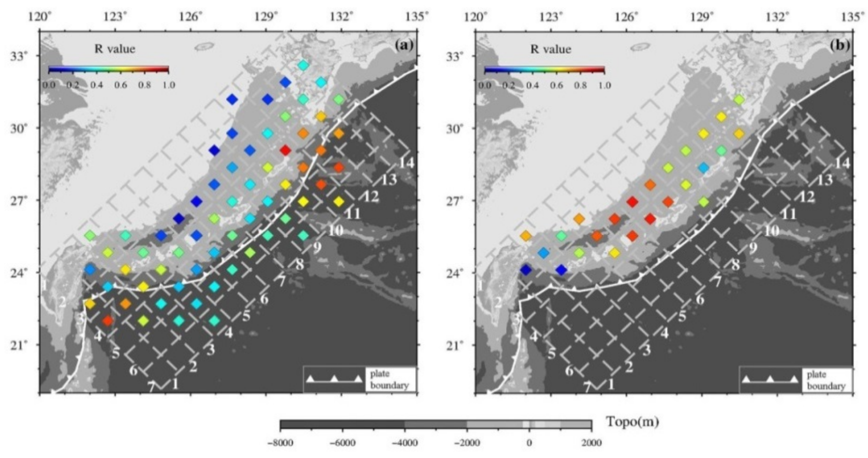

Figure 11. The distribution of the R value: (**a**) shallow stress field; and (**b**) deep stress field.

Table 1. Optimal stress field parameters after inversion of the shallow region.

Range		σ_1 Axis		σ_2 Axis		σ_3 Axis		R
Column	Row	Strike (°)	Dip (°)	Strike (°)	Dip (°)	Strike (°)	Dip (°)	
1	3	168.44	73.45	75.53	0.86	−14.72	16.53	0.51
1	11	70.18	29.12	−138.24	57.65	−27.12	12.85	0.17
2	2	168.38	36.98	71.72	8.76	−29.5	51.64	0.26
2	3	165.12	71.42	−97.55	2.46	−6.73	18.4	0.57
2	4	179.62	75.17	78.81	2.84	−11.93	14.55	0.44
2	9	70.1	17.41	−149.92	67.74	−24.2	13.44	0.09
2	10	80.14	45.5	−124.47	41.78	−22.97	12.57	0.19
2	12	70.84	34.96	−139.45	51.01	−30.02	15.07	0.17
2	13	66.16	21.69	−162.75	58.81	−32.74	21.26	0.2
2	14	77.1	32.07	−163.24	38.31	−39.23	35.3	0.4
3	1	109.98	16.72	−155.9	13.43	−29.02	68.3	0.67
3	2	118.76	25.04	−147.54	7.87	−41.39	63.59	0.33
3	3	127.09	46.25	−119.98	20.45	−13.88	36.64	0.65
3	4	126.9	67.13	−101.89	15.53	−7.21	16.37	0.48
3	5	136.76	80.64	−113.11	3.25	−22.61	8.77	0.19
3	6	70.44	36.45	−128.6	52	−26.51	9.3	0.08
3	7	69.71	26.79	−143.22	58.97	−27.78	14.49	0.12
3	8	62.87	0.41	154.27	73.67	−27.25	16.32	0.21
3	9	−116.32	11.09	116.77	71.93	−23.5	14.09	0.29
3	10	96.13	60.13	−113.37	26.56	−16.92	12.67	0.21
3	11	102.96	50.11	−121.84	30.67	−17.35	22.87	0.38
3	12	108.27	47.9	−133.01	23.48	−26.86	32.64	0.51
3	13	100.02	42.31	−149.46	21.06	−40.42	40.27	0.43
3	14	100.77	33.65	−159.65	14.03	−50.44	52.79	0.37
4	1	110.12	19.3	−149.65	26.88	−11.07	55.94	0.82
4	2	112.42	29.63	−130.31	38.85	−2.95	36.99	0.73
4	3	116.48	31.82	−135	27.11	−13.21	45.82	0.64
4	4	113.98	35.57	−142.8	17.74	−31.24	48.96	0.57
4	5	92.48	25.02	−162.28	29.39	−30.8	49.62	0.49
4	6	87.66	38.17	−130.55	44.98	−19.08	20.12	0.2
4	7	90.11	33.61	−151.35	35.71	−29.29	36.45	0.54
4	8	75.6	19.4	−177.58	39.4	−34.46	44.24	0.41
4	9	73.94	10.88	171.27	33.59	−31.54	54.22	0.36
4	10	110.3	44.4	−139.34	19.56	−32.54	39.14	0.58
4	11	124.91	40.5	−135.81	10.68	−33.93	47.52	0.87
4	12	122.79	35.22	28.94	5.44	−68.66	54.24	0.74
4	13	120.49	40.78	30.13	0.41	−60.34	49.21	0.68
4	14	116.95	33.87	−150.54	3.73	−55.02	55.87	0.5

Table 1. *Cont.*

Range		σ_1 Axis		σ_2 Axis		σ_3 Axis		R
Column	Row	Strike (°)	Dip (°)	Strike (°)	Dip (°)	Strike (°)	Dip (°)	
5	2	107.95	28.36	−106.66	56.74	9.1	15.91	0.57
5	3	107.8	37.54	−100.48	48.89	6.5	14.3	0.39
5	4	100.62	46.12	−117.09	37.26	−11.26	19.72	0.32
5	5	91.05	38.51	−132.86	42.15	−19.42	23.73	0.28
5	6	101.9	52.07	−124.35	28.32	−21.12	23.02	0.32
5	7	97.65	50.64	−131.51	28.21	−27.02	25.01	0.48
5	8	93.36	36.24	−159.18	22.26	−44.65	45.4	0.35
5	9	103.21	44.68	−148.42	17.68	−42.91	40.01	0.37
5	10	125.92	51.46	−142.13	1.55	−50.9	38.5	0.64
5	11	120.52	50.19	28.36	1.8	−63.14	39.75	0.76
5	12	121.09	41.95	24.32	7.48	−73.79	47.07	0.76
5	13	118.75	44.31	28.11	0.65	−62.56	45.68	0.72
6	3	98.89	28.4	−110.05	58.29	1.76	12.93	0.41
6	4	98.37	46.21	−115.75	38.44	−11.08	17.7	0.35
6	5	99.87	50.24	−124.8	30.61	−20.42	22.77	0.37
6	6	102.6	58.55	−122.43	23.37	−23.48	19.8	0.43
6	7	103.5	61.93	−124.88	19.5	−27.73	19.37	0.54
6	8	108.65	47.39	−140.48	18.14	−36.22	36.95	0.44
6	9	103.23	61.04	−138.55	14.66	−41.74	24.38	0.48
6	10	112.73	61.97	−142.42	7.77	−48.47	26.74	0.62
6	11	117.83	56.21	−149.08	2.06	−57.7	33.71	0.8
6	12	118.12	53.23	18.85	6.87	−76.16	35.91	0.81
7	4	96.93	48.79	−118.49	35.51	−15	18.11	0.42
7	9	105.61	61.52	−134.73	15.03	−38	23.59	0.44
7	11	108.56	60.28	−144.44	9.47	−49.38	27.88	0.64

The dip angles of the σ_2 in the mid-to-deep region of the study area are relatively small (2.11–32.71°). In the northern section (rows 11–13), the σ_1 is oriented ESE with dip angles of 24.58–52.62°. The σ_3 is mainly extensional in the WSW direction, and the dip angle is 33.07–48.49°. In the middle and southern sections (rows 4–10), the σ_1 is oriented NNW, and the dip angle is 33.71–65.75°. From north to south, the σ_3 rotates counterclockwise from SW to ENE, with a dip angle of 19.98–49.68°. This is also a high R value region (0.65–0.86), indicating that the σ_1 remains relatively stable. Considering the clockwise rotation of the subducting plate from NNE to ENE from north to south, it is inferred that in the middle and southern sections, the σ_1 is primarily located in the subduction plane and approaches the subduction direction. Additionally, the stress state in this area is compressional in the subduction direction of the subduction zone, and the σ_3 is nearly perpendicular to the subduction plane. The optimal σ_3 in the northern section is extensional along the subduction direction of the subduction zone, and the σ_1 is nearly perpendicular to the subduction plane.

Several studies have revealed that the Ryukyu–Kyushu arc is obviously decoupled and has active back-arc extension [21–23]. Through the above analysis of the stress inversion results of the deep Ryukyu subduction zone, it can be concluded that the deep part of the subduction zone exhibits contrasting characteristics near the Tokara Strait. In the northern part of the Tokara Strait, the dip angle in the deep part of the subduction zone is very steep, the subduction depth is shallow, and the tectonic stress field is extensional along the subduction direction. In the southern part of the Tokara Strait, the dip angle of the subduction zone is relatively gentle, the subduction depth is relatively deep, and the tectonic stress field is compressional along the subduction direction. This difference is related to the speed at which the plates converge and the differences in the physical properties, such as the viscosity and density of the surrounding mantle. In the north, the plate has a low convergence speed. Due to the active volcanism, there are high-temperature and low-viscosity substances in the upper mantle, and the resistance of the plate is small. The plate has negative buoyancy and sinks at a steep dip angle in a tensional state. Conversely, in the central and southern regions, the plates have a high convergence speed, the viscosity of the surrounding mantle is high, the density difference between the mantle and the plate is small, and the plate is subjected to greater resistance. Thus, the plate is subjected to compressional stress and the dip angle is low.

Table 2. Optimal stress field parameters after inversion of the deep region.

Range		σ_1 Axis		σ_2 Axis		σ_3 Axis		R
Column	Row	Strike (°)	Dip (°)	Column	Row	Strike (°)	Dip (°)	
1	3	−74.15	71.72	159.46	11.09	66.58	14.35	0.7
2	2	−110.09	37.26	152.23	9.96	49.72	50.97	0.07
2	3	−139.82	51.68	−39.18	8.3	57.15	37.08	0.28
2	4	−55.2	50.41	−177.2	23.66	78.34	29.67	0.47
2	5	−41.76	47.31	−153.12	18.57	102.34	36.76	0.72
3	3	−75.82	33.71	−171.5	8.44	86.28	54.97	0.13
3	4	−40.26	43.61	−145.69	15.6	109.62	42.24	0.55
3	5	−31.65	43.19	−123.63	2.11	144.12	46.74	0.79
3	6	−34.61	45.9	78.18	20.57	−175.45	36.92	0.82
3	7	−32.27	51.33	102.8	29.54	−153.57	22.58	0.86
3	8	−28.65	53.34	104.13	26.81	−153.47	23.02	0.77
3	9	−20.12	56.55	116.43	25.62	−143.52	19.98	0.57
3	10	5.73	65.75	123.81	11.98	−141.57	20.76	0.56
3	11	95.45	48.49	−14.38	16.71	−117.29	36.66	0.64
3	12	112.3	41.74	−5.24	27.4	−117.34	35.97	0.64
3	13	118.97	33.07	18.62	15.42	−92.55	52.62	0.56
4	5	−29.69	39.25	66.75	7.82	166.06	49.68	0.65
4	6	−33.78	45.11	74.69	17.51	179.86	39.67	0.82
4	7	−32.72	47.72	90.24	26.33	−162.88	30.39	0.85
4	8	−25.98	53.39	95.9	21.43	−161.99	28.13	0.81
4	9	−12.22	57.58	112.97	20.1	−147.52	24.3	0.59
4	10	16.22	63.15	124.16	8.86	−141.65	25.13	0.31
4	11	104.04	42.19	−21.55	32.71	−133.74	30.46	0.48
4	12	108.97	47.7	−24.28	31.95	−130.85	24.58	0.67
5	9	17.53	61.78	122.7	7.99	−143.22	26.87	0.56

In the Okinawa Trough on the inner side of the Ryukyu Island Arc and the deep ocean trench on the outer side of the arc, the extensional axis of the focal mechanism solutions of the shallow earthquakes is mainly perpendicular to the extension direction of the trough and the trench. In the Ryukyu Island Arc, the compression axis is mainly perpendicular to the extension direction of the island arc. As a result, the ocean trough is undergoing NW expansion into a back-arc basin in the same direction as the subduction of the Philippine Sea Plate under the Eurasian Plate. The Ryukyu Island Arc is still under strong NW–SE compressive stress.

The R value of the shallow stress field of the Okinawa Trough is low and the σ_3 is stable in the NNW direction with a small dip angle (>30°). The stress type of the shallow part of the middle and southern sections of the trough transition from strike-slip type to normal fault type reflects the difference in the degree of development of the trough. The southern section of the trough exhibits characteristics that indicate that it is beginning the transformation into an expansion stage. In the coastal trench region to the north of the Tokara Strait, the R value of the shallow stress field is high, and the principal compressive stress is oriented ESE with a large dip angle (>30°).

5. Conclusions

(1) The subduction depth of the Ryukyu Islands subduction zone in the mantle gradually increases from north to south, and the subduction dip angle changes from steep to gentle from north to south. In the northern part of the Tokara Strait, the Benioff zone reaches a maximum depth of 250 km in the mantle, and the Benioff zone bends within a range of 70 km, exhibiting a sagging shape with high subduction dip angles of 70–73°. In the southern part of the Tokara Strait, the maximum depth of the Benioff zone in the mantle is 300 km. The subduction dip angle is gentler near the Tokara Strait than in the north, and the dip angle is about 50–55°. The shape and dip angle of the Benioff zone in the southern part of the Ryukyu Islands subduction zone are gentler, with a dip angle of about 45–50°.

(2) The thrust earthquakes are mainly distributed along the Ryukyu Island Arc. This may be due to the shearing between the subducting plate and the overlying plate, so the earthquakes here are reverse fault type. The normal fault type earthquakes are located in the periphery of the reverse fault type earthquake concentration area, and they spread along the Ryukyu Trench and Okinawa Trough. The subducting plate may bend when it is about to subduct, which leads to stretching of this part of the plate and thus produces the normal fault earthquakes in the trench where the strike of the fault plane is the same as that of the trench. Most of the strike-slip type earthquakes are located in the Okinawa Trough, and a few are scattered in the southeastern part of the Ryukyu Trench, with focal depth of less than 30 km, indicating that there are many oblique faults in the shallow part of the Okinawa Trough.

(3) The tectonic stress field of the Ryukyu Islands subduction zone is extensional along the subduction direction in the northern part of the Tokara Strait and is compressional along the subduction direction in the southern part of the Tokara Strait. This difference is related to the plate convergence speed and the differences in the physical properties, such as the viscosity and density of the surrounding mantle. The subducting plates in the north have a low convergence speed. Due to the active volcanism, there are high-temperature and low-viscosity substances in the upper mantle, and the resistance of the plate is small. The plate has negative buoyancy and sinks at a high dip angle in a tensional state. Conversely, the plates in the central and southern regions have a high convergence speed, the viscosity of the surrounding mantle is high, and the difference between the densities of the mantle and plate is small. The plates are subjected to greater resistance and are therefore subjected to compressive stress.

(4) In the Okinawa Trough on the inner side of the Ryukyu Island Arc and the deep ocean trench on the outer side of the arc, the extensional axis of the focal mechanism solutions of the shallow earthquakes is mainly perpendicular to the extension direction of the trough and the trench. In the Ryukyu Island Arc, the compressive axis is mainly perpendicular to the extension direction of the island arc. Consequently, the ocean trough is carrying out NW expansion into a back-arc basin in the same direction as

the subduction of the Philippine Sea Plate under the Eurasian Plate. The Ryukyu arc is still under strong NW–SE compressive stress. The R value of the shallow stress field of the Okinawa Trough is low, and the σ_3 is stable in the NNW direction with a small dip angle (>30°). The stress field in the shallow part of the Okinawa Trough transitions from strike-slip type to normal fault type from north to south, reflecting the difference in the degree of development of the trough, and the southern segment of the trough is beginning the transition to an expansion stage.

Author Contributions: Z.X. and E.W. contributed to the conceptualization and methodology of the study, formal analysis, and writing—original draft preparation; Z.X. and Y.L. contributed to the project supervision and administration and funding acquisition. All authors have read and agreed to the published version of the manuscript.

Funding: This research was supported by the National Key Research and Development Program of China (2017YFC1500400) and the National Institute of Natural Hazards, Ministry of Emergency Management of China (ZDJ2020-09).

Institutional Review Board Statement: Not applicable.

Informed Consent Statement: Not applicable.

Data Availability Statement: We used the following earthquake catalogs from: the China earthquake catalog for the *National Fifth-Generation Ground Motion Parameter Zoning Map*, and earthquake data from the China Earthquake Data Center (http://data.earthquake.cn/), International Seismological Center ISC (http://www.isc.ac.uk/), National Centers for Environmental Information of National Oceanic and Atmospheric Administration (https://www.ngdc.noaa.gov/),Global Centroid Moment Tensor (https://www.globalcmt.org/CMTsearch.html),Broadband Array in Taiwan for Seismology (BATS)(http://tecws.earth.sinica.edu.tw/BATS). All links accessed on 7 October 2022.

Conflicts of Interest: Author Enhui Wang is employed by the Sinopec Shengli Oilfield Company. The remaining authors declare that the research was conducted in the absence of any commercial or financial relationships that could be construed as a potential conflict of interest.

References

1. Zhang, J.; Li, H.; Chen, Q.; Zhang, H.; Zhou, B. Review on the Research of Subduction Zone. *Geol. Surv. Res.* **2015**, *38*, 18–34. (In Chinese)
2. Muldashev, I.A.; Sobolev, S.V. What controls maximum magnitudes of giant subduction earthquakes? *Geochem. Geophys. Geosystems* **2020**, *21*, e2020GC009145. [CrossRef]
3. Xu, J.-G.; Wu, G.; Feng, D.-C.; Fan, J.-J. Probabilistic multi-hazard fragility analysis of RC bridges under earthquake-tsunami sequential events. *Eng. Struct.* **2021**, *238*, 112250. [CrossRef]
4. Xu, J.; Feng, D.; Mangalathu, S.; Jeon, J. Data-driven rapid damage evaluation for life-cycle seismic assessment of regional reinforced concrete bridges. *Earthq. Engng. Struct. Dyn.* **2022**, *51*, 2730–2751. [CrossRef]
5. Lan, J.-Y.; Liu, J.; Wang, T.; Diwakar, K.; Naqvi, M.W.; Hu, L.-B.; Liu, X.-Q. A centrifuge study on the effect of the water cover on the ground motion of saturated marine sediments. *Soil. Dyn. Earthq. Eng.* **2022**, *152*, 107044. [CrossRef]
6. Lan, J.; Liu, J.; Song, X. Study on the influence of the seafloor soft soil layer on seismic ground motion. *Nat. Hazards Earth Syst. Sci.* **2021**, *21*, 577–585. [CrossRef]
7. Lan, J.; Diwakar, K.; Hu, L.; Gao, Y. An Experimental Study of Dynamic Shear Modulus and Damping Ratio of the Calcareous Sand in the South China Sea. *J. Coast. Res.* **2021**, *37*, 964–972. [CrossRef]
8. Yan, R.; Yan, M.; Yu, H.; Yang, D. Influences of temperature and pore pressure on the geomechanical behaviors of methane hydrate-bearing sand. *Int. J. Geomech.* **2022**, *22*, 04022201. [CrossRef]
9. Yan, R.; Lu, D.; Song, Y.; Yu, H.; Zhang, Q.; Zhou, J. Modeling the Mechanical Behavior of Methane Hydrate-Bearing Soil Considering the Influences of Temperature and Pore Pressure. *Energy Fuels* **2022**, *36*, 12510–12523. [CrossRef]
10. Mamoru, K.; Lynn, R.S. Seismicity and Tectonics of the Western Pacific: Izu-Mariana-Caroline and Ryukyu-Taiwan Regions. *J. Geophys. Res.* **1969**, *74*, 5923–5948.
11. Fitch, T.J. Plate convergence, transcurrent faults and internal deformation adjacent to Southeast Aisa and the western Pacific. *J. Geophys. Res.* **1972**, *77*, 4432–4460. [CrossRef]
12. Shiono, K.; Mikumo, T.; Ishikawa, Y. Tectonics of the Kyushu-Ryukyu arc as evidenced from seismicity and focal mechanism of shallow to intermediate-depth earthquakes. *J. Phys. Earth* **1980**, *28*, 17–43. [CrossRef]
13. Zang, S.; Ning, J.; Xu, L. The distribution of earthquakes, Behavior of the subduction zone and stress state in the Ryukyu island arc. *Acta Seismol. Sin.* **1989**, *11*, 113–123. (In Chinese)

14. Xie, Z.; Li, S.; Lv, Y.; Xu, W.; Zhang, Y.; Liu, W. Unified earthquake catalog for China's seas and adjacent regions and its completeness analysis. *Seismol. Geol.* **2020**, *42*, 993. (In Chinese)
15. Seno, T.; Sakurai, T.; Stein, S. Can the Okhotsk Plate be discriminated from the North American plate? *J. Geophys. Res.* **1996**, *101*, 11305. [CrossRef]
16. Nagamune, T. Intermediate-Depth Earthquakes and Tectonics of the Kyushu-Ryukyu Region. *Zisin* **1987**, *40*, 417–423. [CrossRef]
17. Nagamune, T.; Tashiro, H. Shape of the Wadati-Benioff zone beneath Kyushu, Japan. *J. Seismol. Soc. Jpn.* **1989**, *42*, 13–19.
18. Yakiwara, H.; Shimizu, H.; Miyamachi, H. Three dimensional seismic velocity structure of crust and upper mantle beneath the Kyushu island. *Programme Abstr. Volcanol. Soc. Jpn.* **1996**, *1996*, 143.
19. Hardebeck, J.L.; Michael, A.J. Damped regional-scale stress inversions: Methodology and examples for southern California and the Coalinga aftershock sequence. *J. Geophys. Res. Solid Earth* **2006**, *111*, 310. [CrossRef]
20. Martínez-Garzón, P.; Kwiatek, G.; Ickrath, M.; Bohnhoff, M. MSATSI: A MATLAB Package for Stress Inversion Combining Solid Classic Methodology, a New Simplified User-Handling, and a Visualization Tool. *Seismol. Res. Lett.* **2014**, *85*, 896–904. [CrossRef]
21. Peterson, E.T.; Seno, T. Factors affecting seismic moment release rates in subduction zones. *J. Geophys. Res. Solid Earth* **1984**, *89*, 10233–10248. [CrossRef]
22. Eguchi, T.; Uyeda, S. Seismotectonics of the Okinawa Trough and Ryukyu Arc. *Mem. Geol. Soc. China* **1983**, *5*, 189–210.
23. Kimura, M. Back-arc rifting in the Okinawa Trough. *Mar. Pet. Geol.* **1985**, *2*, 222–240. [CrossRef]